Journal of Cellular Biochemistry 104:202–212 (2008)

Zinc Depletion Efficiently Inhibits Pancreatic Cancer Cell Growth by Increasing the Ratio of Antiproliferative/ Proliferative Genes

M. Donadelli,[1] E. Dalla Pozza,[1] C. Costanzo,[1] M.T. Scupoli,[2] A. Scarpa,[3] and M. Palmieri[1]*

[1]Department of Morphological and Biomedical Sciences, Section of Biochemistry, University of Verona, Verona, Italy
[2]Interdepartmental Laboratory for Medical Research (LURM), University of Verona, Verona, Italy
[3]Department of Pathology, Section of Anatomic Pathology, University of Verona, Verona, Italy

Abstract We investigated the ability of the zinc chelator *N,N,N′,N′*-tetrakis(2-pyridylmethyl)ethylenediamine (TPEN) to reduce pancreatic cancer cell viability. TPEN was much more efficient to inhibit pancreatic adenocarcinoma cell growth than a panel of anti-cancer drugs, including 5-fluorouracil, irinotecan, cisplatin, edelfosine, trichostatin A, mitomycin C, and gemcitabine, the gold standard chemotherapeutic agent for pancreatic cancer. Moreover, TPEN showed a dose- and time-dependent anti-proliferative effect significantly higher on pancreatic cancer cells than on normal primary fibroblasts. This effect may be explained by a significantly higher zinc depletion by TPEN in pancreatic cancer cells as compared to fibroblasts. Cell viability reduction by TPEN was associated to both G1-phase cell cycle arrest and apoptosis, and to the increased ratio of the expression level of cyclin-Cdk inhibitor versus cyclin genes and apoptotic versus anti-apoptotic genes. Finally, we show that apoptotic cell death induced by TPEN involved mitochondrial injury and caspase 3 and caspase 8 activation. In this study, we suggest that zinc depletion may be an efficient strategy in the treatment of pancreatic cancer because of its reduced antiproliferative effect on normal cells. J. Cell. Biochem. 104: 202–212, 2008.

Key words: pancreatic adenocarcinoma; zinc; *N,N,N′,N′*-tetrakis(2-pyridylmethyl)ethylenediamine (TPEN); apoptosis; cell cycle

Zinc is a functionally versatile element with important structural and regulatory roles. It acts as a cofactor for several hundred enzymes [McCall et al., 2000] and facilitates the interaction with DNA of metal-responsive (MTFs) and zinc finger-containing transcription factors. Moreover, zinc modulates the activity of various membrane receptors, transporters, and channels [Hashemi et al., 2007] and regulates specific signal transduction pathways and their target genes by interacting with intracellular signaling molecules [Beyersmann and Haase, 2001]. Because of these essential roles of zinc, cells must maintain a strict intracellular zinc homeostasis, which is accomplished by transporter families and sequestering metallothioneins [Gaither and Eide, 2001; Outten and O'Halloran, 2001; Cousins et al., 2006]. In their physiological state, cells contain a poorly exchangeable amount of zinc that is tightly bound within the tertiary structure of proteins and a dynamic zinc pool subjected to ionic fluxes and readily influenced by zinc deprivation or supplementation [Truong-Tran et al., 2000].

Many reports have shown that both an increase [Kagara et al., 2007] and a decrease [Gupta et al., 2005; Costello and Franklin, 2006] of the zinc level are associated with cancer development. Our group has previously shown that intracellular zinc increase by the ionophore

Grant sponsor: Fondazione Cassa di Risparmio di Verona (Bando 2004); Grant sponsor: Associazione Italiana Ricerca sul Cancro, Milan, Italy; Grant sponsor: Italian Ministries of University—Research and Health; Grant sponsor: European Community; Grant number: PL PL018771; Grant sponsor: Fondazione Giorgio Zanotto, Verona, Italy.

*Correspondence to: Dr. M. Palmieri, Department of Morphological and Biomedical Sciences, Section of Biochemistry, Strada Le Grazie, 8, 37134 Verona, Italy.
E-mail: marta.palmieri@univr.it

Received 16 July 2007; Accepted 21 September 2007
DOI 10.1002/jcb.21613

compound pyrrolidine dithiocarbamate (PDTC) strongly inhibits p53-negative pancreatic cancer cell growth in vitro and in vivo, while it does not affect normal fibroblast proliferation [Donadelli et al., 2006].

The purpose of the present work was to study the effect of the depletion of the endogenous zinc, by using the zinc chelator TPEN, on pancreatic cancer cell and normal fibroblast proliferation and to analyze the molecular mechanisms involved. The antiproliferative efficiency of zinc depletion was compared to that of various chemotherapeutic drugs, including gemcitabine and 5-fluorouracil that represent the standard treatments for pancreatic cancer. We report that TPEN inhibited pancreatic cancer cells, by cell cycle arrest and apoptosis, much more efficiently than a panel of common anti-cancer drugs and showed a significantly higher effect on cancer cells than on normal primary fibroblasts.

MATERIALS AND METHODS

Chemicals

The chemotherapeutic drugs used were: gemcitabine (Gemzar; Eli Lilly), 5-fluorouracil (Teva Pharma), irinotecan (CPT11; Aventis), mitomycin C (Kyowa Italiana Farmaceutici), and cisplatin (Pharmacia). *N*,*N*,*N*′,*N*′-Tetrakis(2-pyridylmethyl)ethylenediamine (TPEN) (Sigma), trichostatin A (Sigma), and edelfosine (Axxora, Alexis) were prepared in absolute ethanol and stored at −80°C until use. Zinc sulfate (Sigma) was prepared in sterile water.

Cell Culture

Human pancreatic adenocarcinoma cell lines (PaCa44, PSN1, HPAF II, PaCa3, T3M4, and CFPAC1; see Moore et al. [2001] for genetic characterization and primary tissue source) were grown in RPMI 1640 supplemented with 20 mM glutamine, 10% FBS, and 50 μg/ml gentamicin sulfate (BioWhittaker) and were incubated at 37°C with 5% CO_2. Normal primary fibroblasts (Promocell PBI) were grown in DMEM supplemented with 20 mM glutamine, 10% FBS, and 50 μg/ml gentamicin sulfate and were incubated at 37°C with 5% CO_2.

Cell Proliferation Assay

Cells were plated in 96-well plates (4×10^3 cells/well) and after 24 h were treated with the indicated compounds. Cells were stained with crystal violet (Sigma) and the dye was solubilized in PBS containing 1% SDS and measured photometrically (A_{595nm}) to determine cell viability.

Cell Cycle Analysis

Cell cycle distribution was analyzed using propidium iodide (PI)-stained cells. Cells were washed with PBS, incubated with 0.1% sodium citrate dihydrate, 0.1% Triton X-100, 200 μg/ml RNase A, 50 μg/ml propidium iodide (Roche Molecular Biochemicals) and analyzed using a flow cytometer (FACScalibur, Becton Dickinson). The percentage of cells in the various stages of the cell cycle was determined using the ModFitLT software.

Apoptosis

The percentage of apoptotic cells was evaluated by staining 2×10^5 cells with annexin V-FITC (Bender Med System) and 5 mg/ml propidium iodide in binding buffer [10 mM HEPES/NaOH (pH 7.4), 140 mM NaOH, and 2.5 mM $CaCl_2$] for 10 min at room temperature in the dark. The samples were analyzed by flow cytometry (FACScalibur, Becton-Dickinson) within 1 h to determine the percentage of cells displaying annexin V^+/propidium $iodide^-$ (early apoptosis) or annexin V^+/propidium $iodide^+$ staining (late apoptosis).

Caspase 3 and caspase 8 activities were assayed by cleavage of the fluorogenic substrates Ac-DEVD-AMC and Ac-IETD-AMC (Biomol), respectively. After the indicated treatments, cells were washed twice with ice-cold PBS and lysed in caspase buffer (100 mM HEPES, 200 mM NaCl, 1 mM EDTA, 20 mM CHAPS, 10% sucrose). Lysates were prepared by repeated freeze-thawing, centrifuged at 14,000*g* for 10 min and the supernatant fraction saved for analysis. One hundred micrograms of total protein extract were incubated with 10 μg of the fluorogenic peptide substrates in a total volume of 800 μl. After a 10 min (caspase 3) or 20 min (caspase 8) incubation at 30°C, the release of 7-amino-4-methylcoumarin was determined fluorometrically, using an excitation wavelength of 380 nm and an emission wavelength of 460 nm. Optimal amounts of cell lysate and duration of assay were determined in preliminary experiments.

Analysis of the Intracellular Zinc Level

Cells (2×10^5) were stained with 2 μM FluoZin-3 (Molecular Probes) at 37°C for 30 min. Before fluorescence measurements, cells were washed in probe-free medium to remove any dye nonspecifically associated and then incubated at 37°C for a further 10 min to allow complete intracellular de-esterification of the probe. Cells were then washed twice in PBS and analyzed by flow cytometry (Ex/Em 494/516 nm).

Analysis of Mitochondrial Membrane Potential ($\Delta\Psi_m$)

Cells (2×10^5) were stained with 40 nM 3, 3-dihexyloxacarbocyanine (Molecular Probes) at 37°C for 20 min and washed twice in PBS. The percentage of cells exhibiting a decreased level of 3,3-dihexyloxacarbocyanine uptake, which reflects loss of $\Delta\Psi_m$, was determined by flow cytometry.

RNA Extraction, RT-PCR, and Image Analysis

Total RNA was extracted from 5×10^6 cells using TRIzol Reagent (Invitrogen) and 1 μg of RNA was reverse transcribed using First Strand cDNA Synthesis for RT-PCR (Invitrogen). For each sample, one-tenth of the cDNAs was used as template for the PCR amplifications using the following primers and cycling conditions: β-*ACTIN*For 5′-ACCAACTGGGACGACATGGAGAA-3′ and β-*ACTIN*Rev 5′-GTGGTGGTGAAGCTGTAGCC-3′, 25 cycles of 94°C for 60 s, 55°C for 60 s and 72°C for 60 s; *BCL-XL*For and *BCL-XS*For 5′-CGGGCATTCAGTGACCTGAC-3′, *BCL-XL*Rev and *BCL-XS*Rev 5′-TCAGGAACCAGCGGTTGAAG-3′, 35 cycles of 94°C for 30 s, 50°C for 30 s and 72°C for 30 s; *BCL-W*For 5′-AAGCTGAGGCAGAAGGGTTA-3′ and *BCL-W*Rev 5′-CCCAAAGACAAAGAAGGCTA-3′, 28 cycles of 94°C for 30 s, 60°C for 30 s and 72°C for 30 s; *P19*For 5′-CTCAACCGCTTCGGCAAGAC-3′ and *P19*Rev 5′-CCTGAAGCAACGTGCACACT-3′, *CYCLINA*For 5′-GCCTGCGTTCACCATTCATG-3′ and *CYCLINA*Rev 5′-CCAGTCCACGAGGATAGCTC-3′, *CYCLINB1*For 5′-AAGAGCTTTAAACTTTGGTCTGGG-3′ and *CYCLINB1*Rev 5′-CTTTGTAAGTCCTTGATTTACCATG-3′, *BCL-2*For 5′-TGCACCTGACGCCCTTCAC-3′ and *BCL-2*Rev 5′-AGACAGCCAGGAGAAATCAAACAG-3′, 30 cycles of 94°C for 30 s, 55°C for 30 s and 72°C for 30 s; *P57*For 5′-TCGCTGCCCGCGTTTGCGCA-3′ and *P57*Rev 5′-CCGAGTCGCTGTCCACTTCGG-3′ 30 cycles of 94°C for 30 s, 60°C for 30 s and 72°C for 30 s. PCR products were separated by electrophoresis through an ethidium bromide-stained 2.0% agarose gel and visualized with ultraviolet light. Gels were photographed and the bands were scanned as digital peaks. The areas of the peaks were calculated in arbitrary units using the public domain NIH Image software (http://rsb.info.nih.gov/nih-image/). The value of β-*ACTIN* mRNA was used as a normalizing factor to evaluate the relative expression levels of the indicated genes.

Statistical Analysis

ANOVA (post hoc Bonferroni) analysis and graphical presentations were performed by GraphPad Prism version 5. *P* values less than 0.05, 0.01, or 0.001 were indicated as *, ** or ***, respectively. Data in Figure 2 were analyzed by paired *t*-test.

RESULTS

TPEN Inhibits Pancreatic Adenocarcinoma Cell Proliferation More Efficiently Than a Panel of Seven Anti-Cancer Drugs

To study the effect of intracellular zinc depletion on pancreatic adenocarcinoma cells, we evaluated both dose- and time-dependent growth inhibition by the zinc chelator TPEN on six cell lines with different origin and genetic profile [Moore et al., 2001] (Fig. 1A,B). We observed that TPEN rapidly (8 h) determined a substantial cell viability inhibition, which was complete at high concentrations and treatment times, suggesting the absence of cell resistance mechanisms. Interestingly, as shown in Figure 2A,B, TPEN treatment was significantly more efficient than a panel of seven anti-cancer drugs (gemcitabine, 5-fluorouracil, irinotecan, cisplatin, edelfosine, trichostatin A, mitomycin C) that are currently used in cancer therapy.

TPEN Is More Effective to Inhibit Cell Growth of Pancreatic Adenocarcinoma Cells Than Normal Primary Fibroblasts

To evaluate the cytotoxic effect of TPEN on normal cells, we compared both dose- and time-dependent proliferation of normal fibroblasts and PaCa44 cells after treatment with TPEN. Figure 3A shows that normal fibroblasts were significantly less sensitive than pancreatic

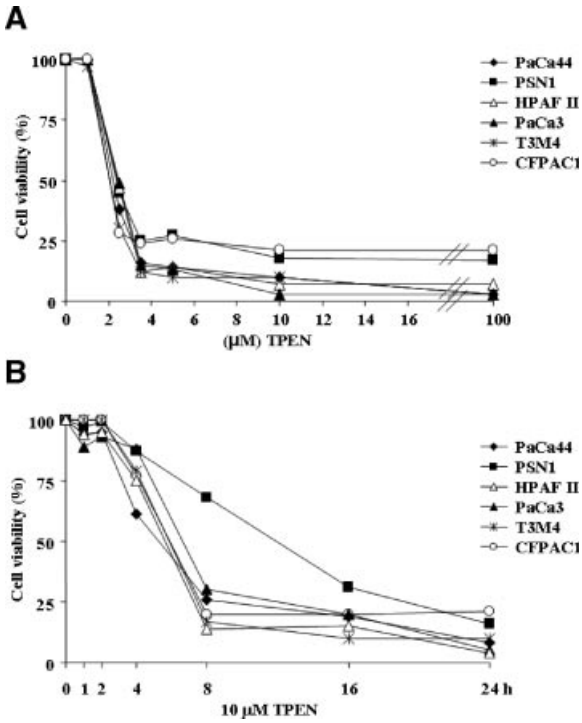

Fig. 1. Effect of TPEN on growth inhibition of a panel of six pancreatic adenocarcinoma cell lines. Cells were seeded in 96-well plates and incubated overnight. TPEN was added at increasing concentrations and cells were further incubated for 24 h (**A**). Cells were treated at the indicated times with 10 μM TPEN (**B**). Cell proliferation was determined using the crystal violet colorimetric assay as described in Materials and Methods Section. Values are the means of triplicate wells from three independent experiments.

adenocarcinoma cells to TPEN treatment. Moreover, normal fibroblasts showed features of cell resistance starting from a TPEN concentration of 10 μM, which was more than sufficient to completely inhibit PaCa44 cell viability. Growth inhibition kinetics in fibroblasts was significantly slower than that obtained in PaCa44 cells, with the highest difference between the two cell types at 8 h (Fig. 3B).

To verify whether the antiproliferative effect of TPEN was due to its chelating activity and did not depend on an unspecific toxicity, we treated cells with TPEN in the absence or presence of supplemented zinc ions in culture medium. We demonstrated that exogenous zinc ions completely counteracted the antiproliferative effect of TPEN both in PaCa44 cells and normal fibroblasts (Fig. 4A). Furthermore, Figure 4B,C shows that TPEN determined an higher intracellular zinc reduction in PaCa44 cells (24 arbitrary units) than in normal fibroblasts (2.7 arbitrary units). This result correlates with the stronger antiproliferative effect of TPEN on PaCa44 cells (see Fig. 3) and may explain the lower sensitivity to TPEN of normal fibroblasts.

TPEN Inhibits Pancreatic Adenocarcinoma Cell Cycle Progression

To examine the molecular mechanisms involved in the inhibition of PaCa44 cell viability by TPEN, we first analyzed cell distribution in the various phases of the cell cycle. Figure 5A shows that TPEN treatment increased the percentage of cells in G1 phase (11% relative to control), while the addition of exogenous zinc ions counteracted TPEN effect. Afterwards, we measured the expression of several genes related to the cell cycle. The intracellular zinc depletion by TPEN induced the expression of *P57* and *P19* tumor suppressor genes and repressed *CYCLIN A* and *CYCLIN B1* (Fig. 5B), while it did not alter the expression of other genes having a function in cell cycle checkpoint such as *P21* and *P27* (data not shown). Figure 5C shows that the ratio of the expression level of the cyclin-cdk inhibitors versus the *CYCLIN* genes was strongly enhanced by TPEN. Thus, TPEN treatment was able to regulate genes involved in both progression and inhibition of the cell cycle thus to determine a global inhibitory effect.

TPEN Induces Apoptotic Cell Death of Pancreatic Adenocarcinoma Cells

Figure 6A shows that TPEN caused PaCa44 apoptotis by increasing the percentage of cells in the early (annexin V^+) and in the late (annexin V^+/propidium $iodide^+$) phases of the apoptotic process. This effect was completely recovered by zinc addition. Analyses of the expression of mitochondrial related apoptotic genes demonstrated that TPEN induced the apoptotic *BCL-X*$_S$ expression, probably by regulating the alternative splicing of *BCL-X*, and inhibited the anti-apoptotic *BCL-2*, *BCL-W*, and *BCL-X*$_L$ (Fig. 6B). Although TPEN did not induce other important apoptotic genes such as *BIM*, *BAK*, *BAX*, *PUMA*, and *NOXA* (data not shown), it is noteworthy that TPEN strongly enhanced (9-fold) the ratio of the expression level of apoptotic versus anti-apoptotic genes (Fig. 6C). Consistently with these results, Figure 6D reports that TPEN treatment increased the percentage of PaCa44 cells having low values of mitochondrial transmembrane

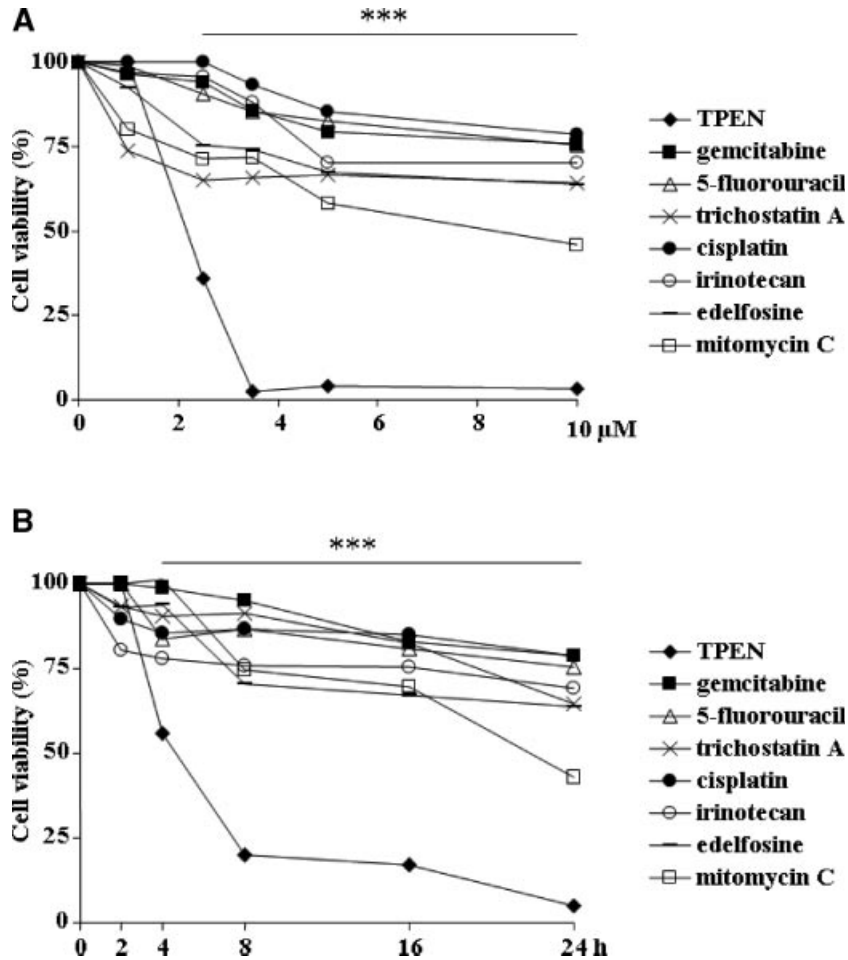

Fig. 2. Pancreatic adenocarcinoma cell growth inhibition by TPEN and chemotherapeutic agents. PaCa44 cells were seeded in 96-well plates and incubated overnight. Drugs were added at increasing concentrations and cells were further incubated for 24 h (**A**). Cells were treated at the indicated times with 10 μM of each drug (**B**). Cell proliferation was determined using the crystal violet colorimetric assay as described in Materials and Methods Section. Values are the means of triplicate wells from three independent experiments. ***$P < 0.001$ (TPEN vs. other drugs).

potential ($\Delta\Psi_m$) and the addition of exogenous zinc ions completely recovered mitochondrial injury. Figure 6E shows that TPEN induced the activity of caspase 3 and caspase 8 (11- and 2.5-fold, respectively), demonstrating their involvement in TPEN-induced apoptotic cell death.

DISCUSSION

We investigated the effect of intracellular zinc chelation on pancreatic adenocarcinoma cell growth. Our results demonstrate that the depletion of zinc ions determines cell cycle arrest and apoptosis via specific regulation of genes involved in both cellular processes. Zinc depletion has already been described to determine cell cycle arrest and apoptosis in numerous cell types [Kolenko et al., 2001; Smith et al., 2002; Hashemi et al., 2007]. Our study reports for the first time that pancreatic adenocarcinoma cell growth is inhibited by zinc depletion and that normal fibroblasts are much less sensitive to the same treatment.

Pancreatic adenocarcinoma is one of the most aggressive human cancers [Neoptolemos et al., 2003]. Standard treatments for advanced disease include chemotherapy with 5-fluorouracil (5-FU) and gemcitabine. However, even gemcitabine, which is now considered the gold standard, has a response rate of less than 20% [Haller, 2003; Li et al., 2004]. A major cause of treatment failure is believed to be resistance to

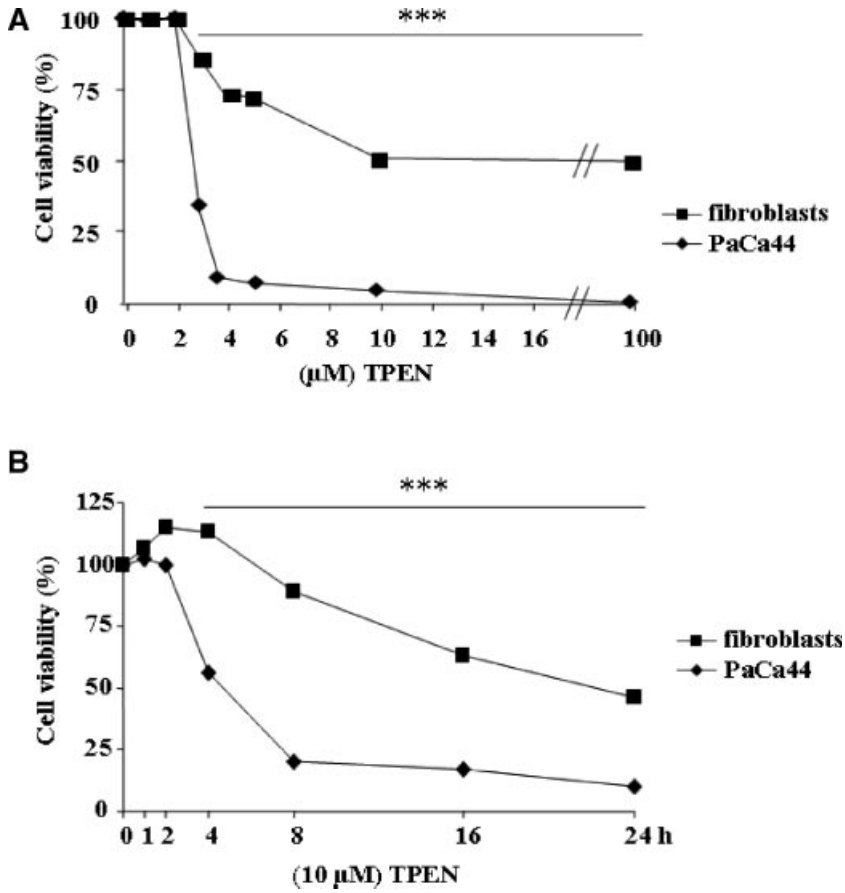

Fig. 3. Effect of TPEN on normal primary fibroblast and pancreatic adenocarcinoma cell viability. PaCa44 cells and normal fibroblasts were treated with increasing concentrations of TPEN for 24 h (**A**) or treated at the indicated times with 10 μM TPEN (**B**). Cell proliferation was determined using the crystal violet colorimetric assay as described in Materials and Methods Section. Values are the means of triplicate wells from three independent experiments. ***$P < 0.001$ (PaCa44 cells vs. fibroblasts).

chemotherapy, which seems to be related to the high frequency of mutation of genes involved in cell growth control, such as *TP53*, *K-RAS*, and *P16* [Moore et al., 2001]. For instance, *TP53* has been shown to increase the sensitivity of pancreatic cancer cells to gemcitabine when reintroduced in these cells [Galmarini et al., 2002]. Thus, the identification of novel drug strategies more effective than gemcitabine-based treatment for pancreatic cancer is a desirable goal. Our dose–response and time-dependent experiments demonstrate that TPEN is much more efficient to inhibit pancreatic cancer cell growth than gemcitabine (a nucleoside analogue of cytidine) and 5-fluorouracil (a base analogue of uracil), and a panel of anti-cancer drugs including irinotecan (a DNA topoisomerase I inhibitor), cisplatin (a DNA cross-linker inhibiting its replication), edelfosine (an alkyl-lysophospholipid), trichostatin A (an histone deacetylase inhibitor), and mitomycin C (an inhibitor of DNA synthesis). Furthermore, we show that cell growth inhibition by TPEN is prevented by the addition of free zinc ions in the culture medium, indicating that TPEN effect is due to its chelating activity and not an unspecific toxicity. Altogether these data may provide a first experimental basis for the establishment of a therapy in pancreatic cancer having as a target zinc homeostasis.

TPEN has previously been demonstrated to induce cell growth inhibition by oxidative stress and *P53* induction [Ho and Ames, 2002; Ho et al., 2003]. Our recent data have shown that in normal fibroblasts a low level of p53 activation is probably responsible for the protection of the cells from PDTC/ROS mediated cellular inhibition [Donadelli et al., 2006], via the induction of the antioxidant gene *SESTRIN 2*. To assess whether p53 activation may have a role also in

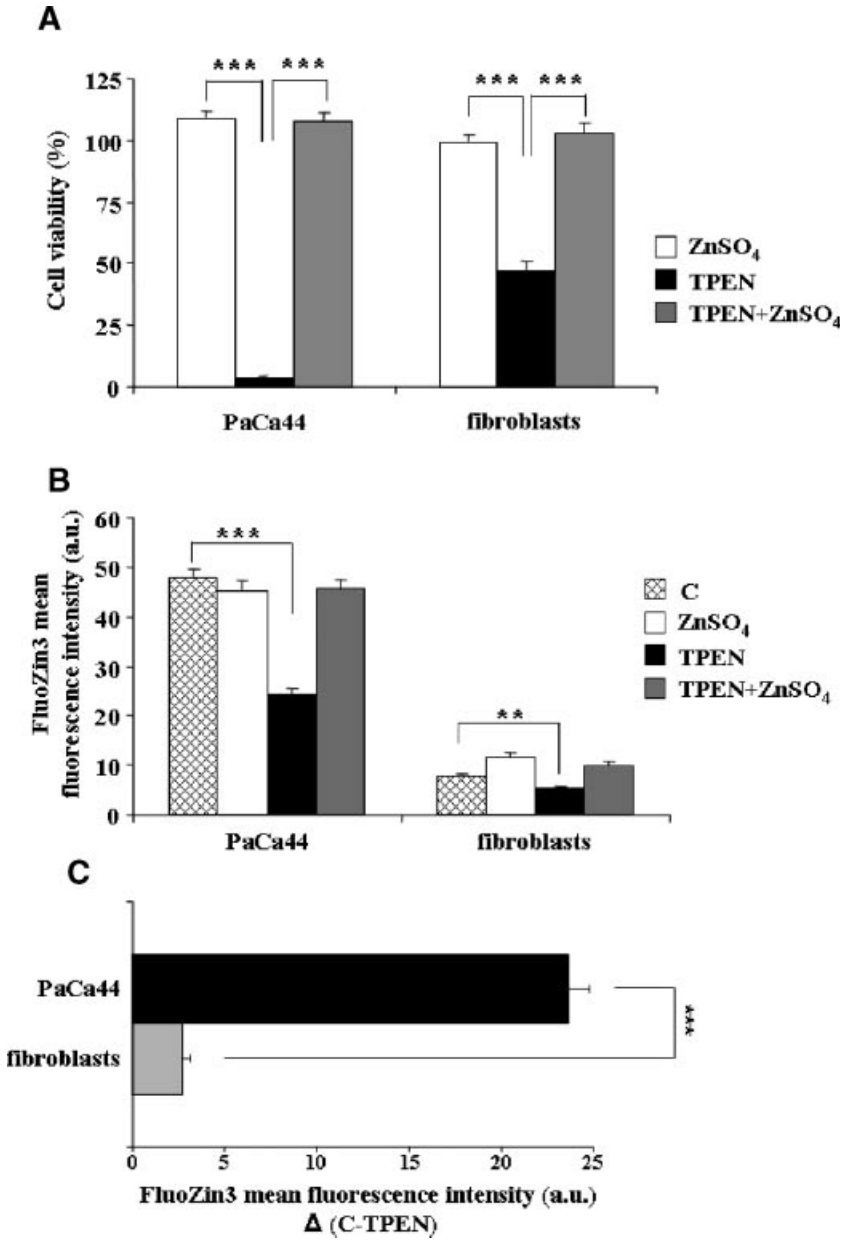

Fig. 4. Effect of TPEN on intracellular zinc levels. **A**: PaCa44 cells and fibroblasts were treated with 10 μM $ZnSO_4$, 10 μM TPEN, or their association for 24 h. Cell proliferation was determined using the crystal violet colorimetric assay as described in Materials and Methods Section. Values are the means of triplicate wells from three independent experiments (±SEM). $^{***}P < 0.001$. **B**: PaCa44 cells and fibroblasts were treated with 10 μM $ZnSO_4$, 10 μM TPEN, or their association for 4 h. The FluoZin3 fluorescence intensity, corresponding to the level of intracellular zinc ions, was measured by flow cytometry as described in Materials and Methods Section. Values are the means of three independent experiments (±SEM). $^{***}P < 0.001$, $^{**}P < 0.01$. **C**: Statistical analysis of data shown in (B). Δ(C-TPEN) represents the difference of the intracellular zinc level before and after TPEN treatment. $^{***}P < 0.001$.

the partial resistance of fibroblasts to TPEN, we treated fibroblasts with TPEN and analyzed (Ser15)-p53 phosphorylation and cell proliferation in the absence or presence of the radical scavenger NAC (*N*-acetyl-L-cysteine). TPEN was neither able to regulate p53 nor to produce ROS, as revealed by the inability of NAC to recover the antiproliferative effect of TPEN (data not shown). Thus, the lower sensitivity to TPEN of fibroblasts compared to pancreatic cancer cells is not determined by p53 activation, but it is probably related to the differential level

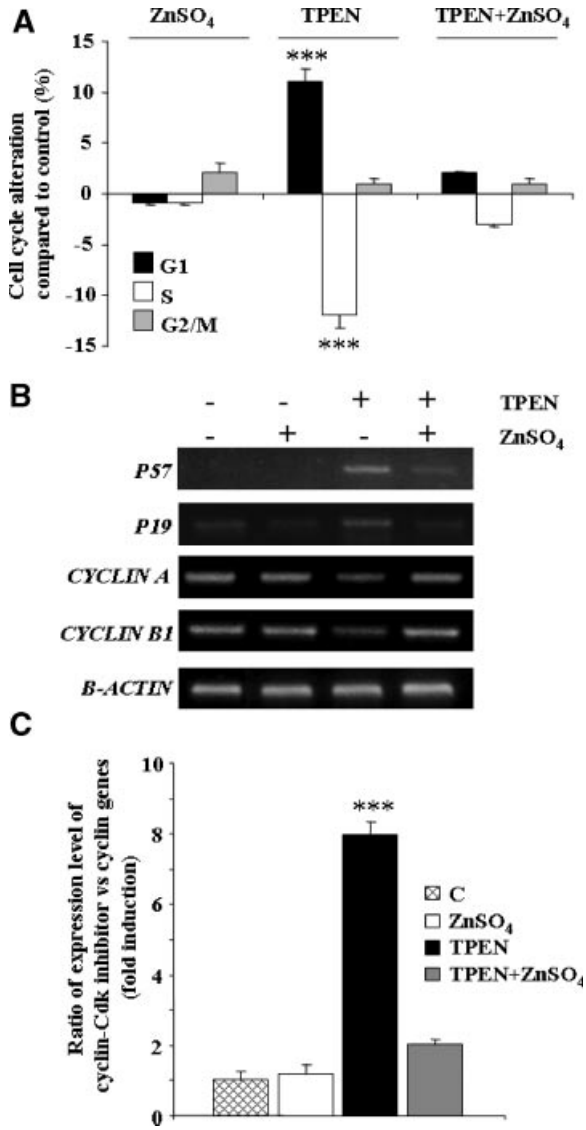

Fig. 5. Effect of TPEN on cell cycle distribution in pancreatic adenocarcinoma cells and cell cycle related gene expression. **A**: PaCa44 cells were treated with 10 μM $ZnSO_4$, 10 μM TPEN, or their association for 24 h. Cell cycle distribution was analyzed by a flow cytometer after DNA staining with propidium iodide. Values are the means of triplicate wells from three independent experiments (±SEM). ***$P < 0.001$. **B**: RT-PCR analysis was performed on total RNA obtained from PaCa44 cells treated with 10 μM $ZnSO_4$, 10 μM TPEN, or their association for 8 h. Primer sequences and PCR conditions are described in Materials and Methods Section. A representative experiment is shown. **C**: Densitometric analysis of *P57*, *P19*, *CYCLIN A*, and *CYCLIN B1* bands normalized to β-*ACTIN*. Fold induction of the expression level ratio of *P57* + *P19*/*CYCLIN A* + *CYCLIN B1* is shown. Values are the means (±SEM) of three independent experiments. ***$P < 0.001$.

of zinc (about ninefold less in fibroblasts) after TPEN treatment.

We report that TPEN treatment of pancreatic adenocarcinoma cells determines cell cycle arrest at G1 phase and increases the ratio of the expression level of cyclin-cdk inhibitor (*P57* and *P19*) versus *CYCLIN* genes (*CYCLIN A* and *CYCLIN B1*). It has been previously demonstrated that the induction of p19 and p57 arrests cell cycle progression at the G1 phase [Schwarze et al., 2001], while cyclin A and cyclin B1 inhibition blocks cell cycle at the S and G2/M and G2/M phases, respectively [Desdouets et al., 1995; Porter and Donoghue, 2003]. Our results demonstrate that TPEN modulates the expression of cell cycle related genes in a way to potentially arrest all phases of the cell cycle. However, we report that TPEN arrests cells only at the G1 phase. To explain this apparent contradiction, we may speculate that TPEN, indeed, blocks the cycle at any phase, but we may appreciate only the arrest at the G1 phase, probably due to a prevalent contribution of *P19* and *P57* induction, because the cell cycle alteration is measured as a percentage value. In addition, we report that TPEN is not able to regulate other genes involved in cell cycle control, such as *P21* and *P27* (data not shown), indicating that the process is specific. These results suggest that zinc depletion may specifically affect the activity of zinc dependent transcriptional activators and repressors of genes that control cell cycle. The regulation of cell cycle-related genes by TPEN could assume a great relevance in pancreatic cancer, which presents a high frequency of mutations in *P16* and *P15* [Naumann et al., 1996].

Apoptotic analyses show that TPEN is also able to induce a strong apoptotic cell death in pancreatic cancer cells, which is completely recovered by the addition of exogenous zinc ions. The apoptotic feature has been confirmed by the detection of nucleosomes in the cytoplasmic fraction of pancreatic cancer cells treated with TPEN (data not shown). Intracellular zinc depletion increases the ratio of the expression level of apoptotic/antiapoptotic mitochondrial-related Bcl-2 genes, enhances the percentage of pancreatic cancer cells harboring a low mitochondrial transmembrane potential, and activates caspase 3 and caspase 8. Since pro- and anti-apoptotic Bcl-2 family members are known to function in coordination for the regulation of the apoptotic machinery and their relative levels are critical for cell fate, we believe that the increased ratio of apoptotic/antiapoptotic gene expression may be crucial for the apoptotic

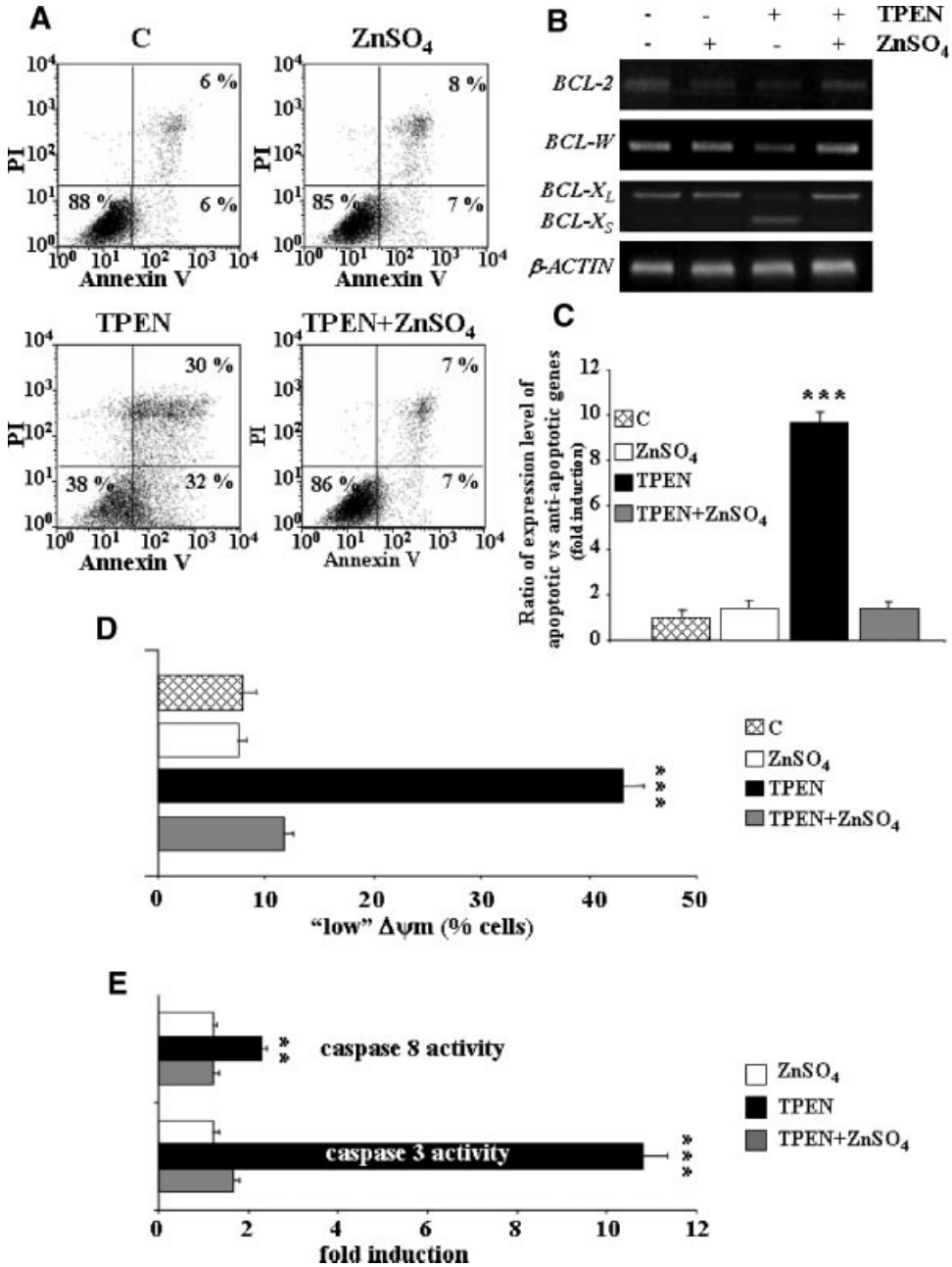

Fig. 6. Apoptotic cell death in pancreatic adenocarcinoma cells treated with TPEN. **A**: PaCa44 cells were treated with 10 μM $ZnSO_4$, 10 μM TPEN, or their association for 16 h. 2×10^5 cells were analyzed by flow cytometry to determine the percentage of cells displaying annexin V^+/propidium $iodide^-$ (early apoptosis) or annexin V^+/propidium $iodide^+$ staining (late apoptosis). Values of a representative experiment are shown. **B**: RT-PCR analysis was performed on total RNA obtained from PaCa44 cells treated with 10 μM $ZnSO_4$, 10 μM TPEN, or their association for 8 h. Primer sequences and PCR conditions are described in Materials and Methods Section. A representative experiment is shown. **C**: Densitometric analysis of *BCL-2*, *BCL-W*, *BCL-X_L*, and *BCL-X_S* bands normalized to β-*ACTIN*. Fold induction of the expression level ratio of *BCL-X_S*/*BCL-2* + *BCL-W* + *BCL-X_L* is shown. Values are the means (±SEM) of three independent experiments. $^{***}P < 0.001$. **D**: PaCa44 cells were treated with 10 μM $ZnSO_4$, 10 μM TPEN, or their association for 16 h and the percentage of cells exhibiting reduced $\triangle\Psi_m$ was determined by flow cytometry using 3,3-dihexyloxacarbocyanine staining as described in Materials and Methods Section. Values are the means of three independent experiments (±SEM). $^{***}P < 0.001$. **E**: Caspase 8 and caspase 3 activities in PaCa44 cells treated with 10 μM $ZnSO_4$, 10 μM TPEN, or their association for 16 h. Caspase activities were assessed as described in the Materials and Methods Section. Values are the means of three independent experiments (±SEM). $^{***}P < 0.001$, $^{**}P < 0.01$.

induction by TPEN. However, as zinc has been shown to inhibit caspase 3 activation [Takahashi et al., 1996], a direct stimulation of caspase 3 proteolytic processing by zinc depletion may also contribute to TPEN induced cell death in pancreatic cancer cells. Caspase 8 activation, which could represent a mere consequence of caspase 3 activation [Chimienti et al., 2001], may also have a role in TPEN mediated apoptosis.

Metal chelators are currently used in clinical trials. Antitumoral activity of ICRF-159, a chelator of divalent cations, has been demonstrated in patients with a variety of tumor types including non-small cell lung cancer [Eagan et al., 1976], colorectal carcinoma [Marciniak et al., 1975; Bellet et al., 1976], Kaposi's sarcoma [Olweny et al., 1976], non-Hodgkin's lymphoma [Flannery et al., 1978], acute leukemia [Bakowski et al., 1979], and head and neck carcinoma [Shah et al., 1982]. Phase I studies of dexrazoxane, a bidentate chelator that resembles EDTA, have been performed using a variety of dosing schedules. Interestingly, the maximal tolerated dose (MTD) of dexrazoxane determined by using short infusion schedules was approximately 10–15 times higher than the MTD determined with continuous infusion schedules [Tetef et al., 2001]. Myelosuppression appeared as the strongest toxic effect and was used to established the limiting dose of metal chelators [Tetef et al., 2001; Chow et al., 2004]. Thus, in planning a therapy with this class of agents, the infusion schedule must be carefully evaluated.

In this work, we demonstrate that TPEN efficiently inhibits pancreatic adenocarcinoma cell growth providing opportunities for developing potential pharmacological approaches to inhibit pancreatic cancer growth in vivo.

REFERENCES

Bakowski MT, Prentice HG, Lister TA, Malpas JS, McElwain TJ, Powles RL. 1979. Limited activity of ICRF-159 in advanced acute leukemia. Cancer Treat Rep 63:127–129.

Bellet RE, Engstrom PF, Catalano RB, Creech RH, Mastrangelo MJ. 1976. Phase II study of ICRF-159 in patients with metastatic colorectal carcinoma previously exposed to systemic chemotherapy. Cancer Treat Rep 60: 1395–1397.

Beyersmann D, Haase H. 2001. Functions of zinc in signaling, proliferation and differentiation of mammalian cells. Biometals 14:331–341.

Chimienti F, Seve M, Richard S, Mathieu J, Favier A. 2001. Role of cellular zinc in programmed cell death: Temporal relationship between zinc depletion, activation of caspases, and cleavage of Sp family transcription factors. Biochem Pharmacol 62:51–62.

Chow WA, Synold TW, Tetef ML, Longmate J, Frankel P, Lawrence J, Al-Khadimi Z, Leong L, Lim D, Margolin K, Morgan RJ, Jr., Raschko J, Shibata S, Somlo G, Twardowski P, Yen Y, Doroshow JH. 2004. Feasibility and pharmacokinetic study of infusional dexrazoxane and dose-intensive doxorubicin administered concurrently over 96 h for the treatment of advanced malignancies. Cancer Chemother Pharmacol 54:241–248.

Costello LC, Franklin RB. 2006. The clinical relevance of the metabolism of prostate cancer; zinc and tumor suppression: Connecting the dots. Mol Cancer 5:17.

Cousins RJ, Liuzzi JP, Lichten LA. 2006. Mammalian zinc transport, trafficking, and signals. J Biol Chem 281: 24085–24089.

Desdouets C, Sobczak-Thepot J, Murphy M, Brechot C. 1995. Cyclin A: Function and expression during cell proliferation. Prog Cell Cycle Res 1:115–123.

Donadelli M, Dalla Pozza E, Costanzo C, Scupoli MT, Piacentini P, Scarpa A, Palmieri M. 2006. Increased stability of P21(WAF1/CIP1) mRNA is required for ROS/ERK-dependent pancreatic adenocarcinoma cell growth inhibition by pyrrolidine dithiocarbamate. Biochim Biophys Acta 1763:917–926.

Eagan RT, Carr DT, Coles DT, Rubin J, Frytak S. 1976. ICRF-159 versus polychemotherapy in non-small cell lung cancer. Cancer Treat Rep 60:947–948.

Flannery EP, Corder MP, Sheehan WW, Pajak TF, Bateman JR. 1978. Phase II study of ICRF-159 in non-Hodgkin's lymphomas. Cancer Treat Rep 62:465–467.

Gaither LA, Eide DJ. 2001. Eukaryotic zinc transporters and their regulation. Biometals 14:251–270.

Galmarini CM, Clarke ML, Falette N, Puisieux A, Mackey JR, Dumontet C. 2002. Expression of a non-functional p53 affects the sensitivity of cancer cells to gemcitabine. Int J Cancer 97:439–445.

Gupta SK, Singh SP, Shukla VK. 2005. Copper, zinc, and Cu/Zn ratio in carcinoma of the gallbladder. J Surg Oncol 91:204–208.

Haller DG. 2003. New perspectives in the management of pancreas cancer. Semin Oncol 30:3–10.

Hashemi M, Ghavami S, Eshraghi M, Booy EP, Los M. 2007. Cytotoxic effects of intra and extracellular zinc chelation on human breast cancer cells. Eur J Pharmacol 557:9–19.

Ho E, Ames BN. 2002. Low intracellular zinc induces oxidative DNA damage, disrupts p53, NFkappa B, and AP1 DNA binding, and affects DNA repair in a rat glioma cell line. Proc Natl Acad Sci USA 99:16770–16775.

Ho E, Courtemanche C, Ames BN. 2003. Zinc deficiency induces oxidative DNA damage and increases p53 expression in human lung fibroblasts. J Nutr 133: 2543–2548.

Kagara N, Tanaka N, Noguchi S, Hirano T. 2007. Zinc and its transporter ZIP10 are involved in invasive behavior of breast cancer cells. Cancer Sci 98:692–697.

Kolenko VM, Uzzo RG, Dulin N, Hauzman E, Bukowski R, Finke JH. 2001. Mechanism of apoptosis induced by zinc deficiency in peripheral blood T lymphocytes. Apoptosis 6:419–429.

Li D, Xie K, Wolff R, Abbruzzese JL. 2004. Pancreatic cancer. Lancet 363:1049–1057.

Marciniak TA, Moertel CG, Schutt AJ, Hahn RG, Reitemeier RJ. 1975. Phase II study of ICRF-159 (NSC-129943) in advanced colorectal carcinoma. Cancer Chemother Rep 59:761–763.

McCall KA, Huang C, Fierke CA. 2000. Function and mechanism of zinc metalloenzymes. J Nutr 130:1437S–1446S.

Moore PS, Sipos B, Orlandini S, Sorio C, Real FX, Lemoine NR, Gress T, Bassi C, Kloppel G, Kalthoff H, Ungefroren H, Lohr M, Scarpa A. 2001. Genetic profile of 22 pancreatic carcinoma cell lines. Analysis of K-ras, p53, p16 and DPC4/Smad4. Virchows Arch 439:798–802.

Naumann M, Savitskaia N, Eilert C, Schramm A, Kalthoff H, Schmiegel W. 1996. Frequent codeletion of p16/MTS1 and p15/MTS2 and genetic alterations in p16/MTS1 in pancreatic tumors. Gastroenterology 110:1215–1224.

Neoptolemos JP, Cunningham D, Friess H, Bassi C, Stocken DD, Tait DM, Dunn JA, Dervenis C, Lacaine F, Hickey H, Raraty MG, Ghaneh P, Buchler MW. 2003. Adjuvant therapy in pancreatic cancer: Historical and current perspectives. Ann Oncol 14:675–692.

Olweny CL, Masaba JP, Sikyewunda W, Toya T. 1976. Treatment of Kaposi's sarcoma with ICRF-159 (NSC-129943). Cancer Treat Rep 60:111–113.

Outten CE, O'Halloran TV. 2001. Femtomolar sensitivity of metalloregulatory proteins controlling zinc homeostasis. Science 292:2488–2492.

Porter LA, Donoghue DJ. 2003. Cyclin B1 and CD K1:nuclear localization and upstream regulators. Prog Cell Cycle Res 5:335–347.

Schwarze SR, Shi Y, Fu VX, Watson PA, Jarrard DF. 2001. Role of cyclin-dependent kinase inhibitors in the growth arrest at senescence in human prostate epithelial and uroepithelial cells. Oncogene 20:8184–8192.

Shah MK, Engstrom PF, Catalano RB, Paul AR, Bellet RE, Creech RH. 1982. Phase II trial of razoxane (ICRF-159) in patients with squamous cell carcinoma of the head and neck previously exposed to systemic chemotherapy. Cancer Treat Rep 66:557–558.

Smith PJ, Wiltshire M, Davies S, Chin SF, Campbell AK, Errington RJ. 2002. DNA damage-induced [Zn(2+)](i) transients: Correlation with cell cycle arrest and apoptosis in lymphoma cells. Am J Physiol Cell Physiol 283: C609–C622.

Takahashi A, Alnemri ES, Lazebnik YA, Fernandes-Alnemri T, Litwack G, Moir RD, Goldman RD, Poirier GG, Kaufmann SH, Earnshaw WC. 1996. Cleavage of lamin A by Mch2 alpha but not CP P32: Multiple interleukin 1 beta-converting enzyme-related proteases with distinct substrate recognition properties are active in apoptosis. Proc Natl Acad Sci USA 93:8395–8400.

Tetef ML, Synold TW, Chow W, Leong L, Margolin K, Morgan R, Raschko J, Shibata S, Somlo G, Yen Y, Groshen S, Johnson K, Lenz HJ, Gandara D, Doroshow JH. 2001. Phase I trial of 96-hour continuous infusion of dexrazoxane in patients with advanced malignancies. Clin Cancer Res 7:1569–1576.

Truong-Tran AQ, Ho LH, Chai F, Zalewski PD. 2000. Cellular zinc fluxes and the regulation of apoptosis/gene-directed cell death. J Nutr 130:1459S–1466S.